ACCOUNTS of chemical research

pubs.acs.org/accounts Article

Electrochemical Gelation of Metal Chalcogenide Quantum Dots: Applications in Gas Sensing and Photocatalysis

Published as part of the Accounts of Chemical Research special issue "Electrosynthesis of Inorganic Materials".

Xin Geng,‡ Daohua Liu,‡ Chathuranga C. Hewa-Rahinduwage, Stephanie L. Brock,* and Long Luo*

Cite This: *Acc. Chem. Res.* 2023, 56, 1087−1096 Read Online

CONSPECTUS: Metal chalcogenide quantum dots (QDs) are prized for their unique and functional properties, associated with both intrinsic (quantum confinement) and extrinsic (high surface area) effects, as dictated by their size, shape, and surface characteristics. Thus, they have considerable promise for diverse applications, including energy conversion (thermoelectrics and photovoltaics), photocatalysis, and sensing. QD gels are macroscopic porous structures consisting of interconnected QDs and pore networks in which the pores may be filled with solvent (i.e., wet gels) or air (i.e., aerogels). QD gels are unique because they can be prepared as macroscale objects while fully retaining the size-specific quantum-confined properties of the initial QD building blocks. The extensive porosity of the gels also ensures that each QD in the gel network is accessible to the ambient, leading to high performance in applications that require high surface areas, such as (photo)catalysis and sensing.

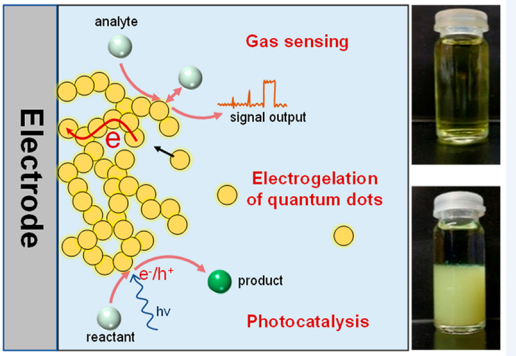

Metal chalcogenide QD gels are conventionally prepared by chemical approaches. We recently expanded the toolbox for QD gel synthesis by developing electrochemical gelation methods. Relative to conventional chemical oxidation approaches, electrochemical assembly of QDs (1) enables the use of two additional levers for tuning the QD assembly process and gel structure: electrode material and potential, and (2) allows direct gel formation on device substrates to simplify device fabrication and improve reproducibility. We have discovered two distinct electrochemical gelation methods, each of which enables the direct writing of gels on an active electrode surface or the formation of free-standing monoliths. Oxidative electrogelation of QDs leads to assemblies bridged by dichalcogenide (covalent) linkers, whereas metal-mediated electrogelation proceeds via electrodissolution of active metal electrodes to produce free ions that link QDs by binding to pendant carboxylate functionalities on surface ligands (non-covalent linkers). We further demonstrated that the electrogel composition produced from the covalent assembly could be modified by controlled ion exchange to form single-ion decorated bimetallic QD gels, a new category of materials. The QD gels exhibit unprecedented performance for NO_2 gas sensing and unique photocatalytic reactivities (e.g., the "cyano dance" isomerization and the reductive ring-opening arylation). The chemistry unveiled during the development of electrochemical gelation pathways for QDs and their post-modification has broad implications for guiding the design of new nanoparticle assembly strategies and QD gel-based gas sensors and catalysts.

KEY REFERENCES

- Hewa-Rahinduwage, C.; Geng, X.; Silva, K. L.; Niu, X.; Zhang, L.; Brock, S. L.; Luo, L. Reversible Electrochemical Gelation of Metal Chalcogenide Quantum Dots. *J. Am. Chem. Soc.* **2020**, *142* (28), 12207−12215.[1] *A facile electrochemical gelation method for oxidation-induced assembly of metal chalcogenide quantum dots into macroscale 3-D connected pore-matter nanoarchitectures, and the use of this method for fabrication of CdS gel gas sensors with exceptional NO_2 sensing performance, is reported.*
- Hewa-Rahinduwage, C.; Silva, K. L.; Brock, S. L.; Luo, L. Quantum Dot Gelation Driven by Electrochemically Generated Metal-ion Crosslinkers,. *Chem. Mater.* **2021**, *33* (12), 4522−4528.[2] *This paper reports an orthogonal approach to electrochemically induced quantum dot assembly by oxidation of a metal electrode to liberate cations that subsequently bridge pendant carboxylate groups on the nanoparticles and the ability to pattern gels onto a printed circuit board chip.*

Received: January 22, 2023
Published: April 20, 2023

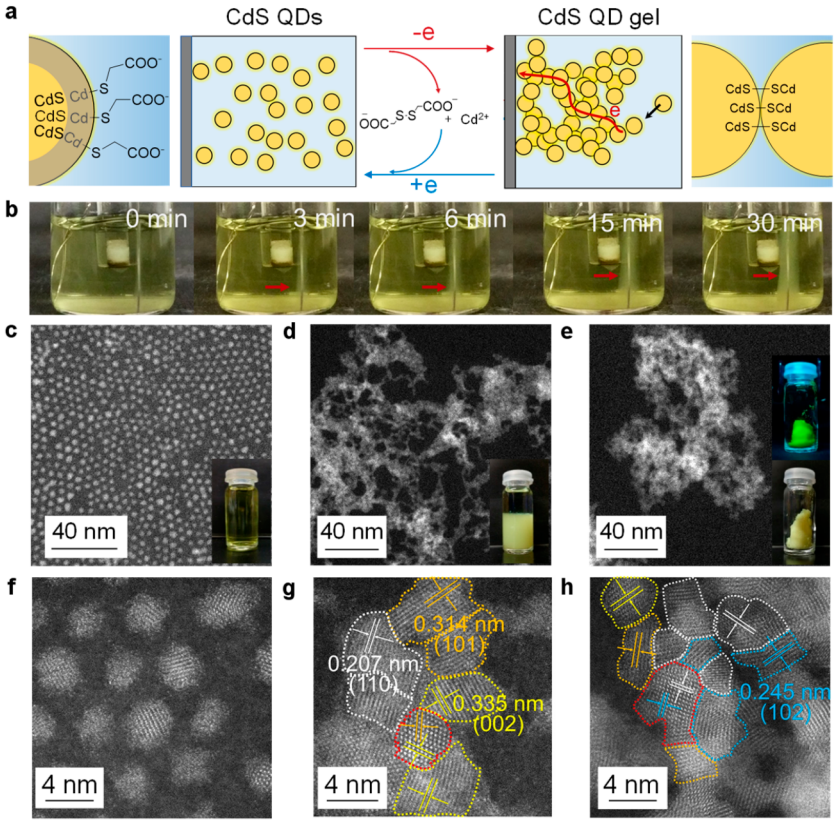

Figure 1. Electrogelation of CdS QDs. **a**, Schematic of the reversible electrogelation mechanism for CdS QDs. **b**, CdS gel growth on a Pt wire electrode as a function of electrogelation time at an electrode potential of 1.2 V vs Ag/AgCl/sat. KCl electrode. **c**–**e**, Low-magnification STEM and TEM images of CdS QDs, wet gel, and aerogel, respectively. The insets show their corresponding photographs. Insets in panel e show a free-standing CdS aerogel under ultraviolet (top) and normal light (bottom). **f**–**h**, High-resolution STEM images of CdS QDs, wet gel, and aerogel, respectively. Crystallites in the gel are color-coded according to their lattice fringes. Reproduced with permission from ref 1. Copyright 2020 American Chemical Society.

- Geng, X.; Li, S.; Mawella-Vithanage, L.; Ma, T.; Kilani, M.; Wang, B.; Ma, L.; Hewa-Rahinduwage, C.; Shafikova, A.; Nikolla, E.; Mao, G.; Brock, S. L.; Zhang, L.; Luo, L. Atomically dispersed Pb ionic sites in PbCdSe quantum dot gels enhance room-temperature NO_2 sensing. *Nat. Commun.* **2021**, *12*, 4895.[3] *Pb(II) cation-exchange of CdSe gels deposited electrochemically by oxidation-induced assembly produces bimetallic PbCdSe quantum dot gels containing atomically dispersed Pb ionic sites, resulting in enhanced NO_2 sensing due to the optimal combination of strong sensor response and fast recovery.*
- Liu, D.; Nyakuchena, J.; Maity, R.; Geng, X.; Mahajan, J.; Hewa-Rahinduwage, C. C.; Peng, Y.; Huang, J.; Luo, L. Quantum Dot Gels as Efficient and Unique Photocatalysts for Organic Synthesis. *Chem. Commun.* **2022**, *58*, 11260–11263.[4] *CdS quantum dot gels are demonstrated to be highly efficient and unique photocatalysts for organic synthesis relative to CdS QDs because of the high accessibility of its surface sites to the substrates and unique surface interactions with the substrates or intermediates.*

INTRODUCTION

Metal chalcogenide (sulfide, selenide, and telluride) semiconductors exhibit a range of properties that lend themselves to existing and potential applications in energy storage, photovoltaics, catalysis, and sensing. Due to quantum confinement effects, the electrooptical properties of metal chalcogenides can be tuned by limiting their size in one or more dimensions to be smaller than the Bohr exciton radius, which ranges from a few nm to a few 10s of nm, depending on the chemical composition and the dimensionality of the confinement (3-D, 2-D, 1-D). Thus, the bandgap can be modified to facilitate optical absorption for, e.g., the solar spectrum (photovoltaics, photocatalysis) or optical emission for light-emitting diodes, with the largest tunability achieved for 3-D confined systems: quantum dots (QDs). Moreover, because of their finite sizes, QDs have large surface/volume ratios relative to bulk systems, which makes them advantageous for applications that benefit from large surface areas, including catalysis and sensing. While surface areas are theoretically maximized in such dispersions, disruption of electrostatic forces can lead to uncontrolled aggregation. The use of bulky surface ligands confers excellent stability in this regard, but limits access of molecules to the active surface. Regardless of the dispersion forces' nature, separating particles limits interparticle communication via carrier transport pathways. One approach to designing stable colloidal systems with robust transport pathways and large surface areas is to aggregate them in a controlled fashion, leading to a macroscale gel with a three-dimensionally connected matter–pore network that preserves the quantum confinement characteristics of the components while enabling electronic/ionic communication and maximizing the exposure of active surface sites to the

https://doi.org/10.1021/acs.accounts.3c00042
Acc. Chem. Res. 2023, 56, 1087–1096

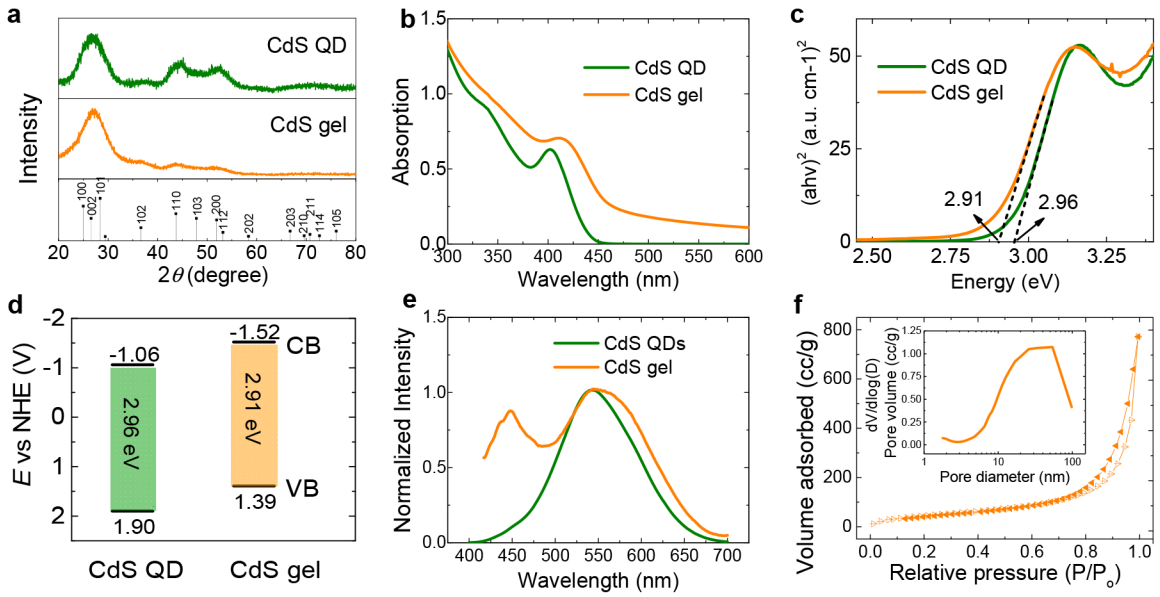

Figure 2. Structural and electronic property characterization of CdS QDs and electrogel. **a**, Powder X-ray diffraction patterns. The stick diagram shows the diffraction pattern of hexagonal CdS as a reference. **b**, UV−visible absorption spectra. **c**, Tauc plot estimated from UV−vis spectra. **d**, Bandgap structure estimated from UV−vis spectra and ultraviolet photoelectron spectroscopy. Reproduced with permission from ref 4. Copyright 2022 Royal Society of Chemistry. **e**, Photoluminescence spectra. **f**, Nitrogen adsorption−desorption isotherm (inset: pore size distribution plot). Reproduced with permission from ref 1. Copyright 2020 American Chemical Society.

environment.[5−7] In such a case, the nature of the interparticle interfaces (covalent or non-covalent) is an essential contributor to the functional properties of the gel.

Covalent attachment can occur via an oxidative process that results in gel structures linked by embedded dichalcogenide linkers (static) or dynamic covalent linkers that bridge pendant groups on the surface ligands of the nanoparticles.[8−10] The first report of a QD gel produced by chemical oxidation was by Gacoin et al., who reported that oxidation of thiolate-capped CdS QDs produced a gel that maintained the quantum confinement properties of the primary particles. They also proposed a mechanism whereby oxidation of surface thiolates leads to irreversible loss of surface ligands as disulfides, followed by progressive aggregation of naked QDs to minimize the total surface energy, leading to gelation.[11,12] Subsequently, the Brock lab capitalized on this discovery, demonstrating the generality of this process across diverse chalcogenide QDs and the ability to dry monolithic wet gels, without loss of porosity, by supercritical processing into aerogels. Brock also clarified the mechanism of oxidative assembly, which does not occur by simple aggregation of deprotected QDs, but rather is driven by oxidation of exposed lattice chalcogenide ions that results in the formation of dichalcogenide bonds between particles.[10] These embedded linkers can be cleaved by chemical reduction, producing a sol in which the QDs have all decreased modestly in size, in keeping with a gelation mechanism that is not truly reversible, as the process of gelation and re-dispersion etches off a surface layer of metal chalcogenide with each cycle. Despite susceptibility to reductive dispersion, the gel network is robust for electrical transport, with electrical conductivities of 10^{-3} S/cm and photocurrent densities of ∼200 μA/cm^2 reported for CdSe QD films prepared via oxidative assembly.[13,14]

Non-covalent interactions can also be used to drive the gelation of metal chalcogenide QDs and other nanoparticles. In this case, control of the repulsive and attractive forces between colloidal NPs in solution progressively reduces the repulsive forces (e.g., steric or electrostatic) until they are overcome by the attractive ones (e.g., van der Waals forces, hydrophobic/hydrophilic interactions, electrostatic).[9] Such control can also be achieved by crosslinkers such as metal ions,[15] polymers,[8,16] and dihydrazide/aldehyde pairs,[9] or by simply freeze-drying a colloidal NP solution.[17,18] The properties of the assemblies are highly dependent on the type of non-covalent interaction and the density of the gels.

In this Account, we discuss our contribution to metal chalcogenide gel formation using electrochemical methods to drive covalent or non-covalent assembly, which enables direct writing on an active electrode surface or formation of free-standing monoliths, and the application of such materials in sensing and photocatalysis.[1−4,19,20] Relative to conventional chemical approaches, electrochemical gelation of metal chalcogenide QDs enables the use of two additional levers for tuning the assembly process: electrode material and potential, allowing the controlled synthesis of complicated gel structures that are challenging to achieve using chemical means. The current challenges and prospects in this field are also briefly discussed.

■ ELECTROCHEMICAL OXIDATIVE GELATION OF QDs (COVALENT ASSEMBLY)

Based on the prior work by the Brock group revealing the active role played by chemical oxidants in QD gelation, we proposed that it should be possible to drive similar oxidative gelation of QDs *electrochemically*, particularly because the formed gel network is electrically conductive, which will enable the electooxidative gelation process to continue beyond the gel−electrode interface.[1] As proof of principle, we studied electrogelation of CdS QDs as a model system (Figure 1), hypothesizing a pathway as shown in Figure 1a (the detailed mechanism is discussed in the next section). We first synthesized CdS QDs by standard hot-injection methods

https://doi.org/10.1021/acs.accounts.3c00042
Acc. Chem. Res. 2023, 56, 1087−1096

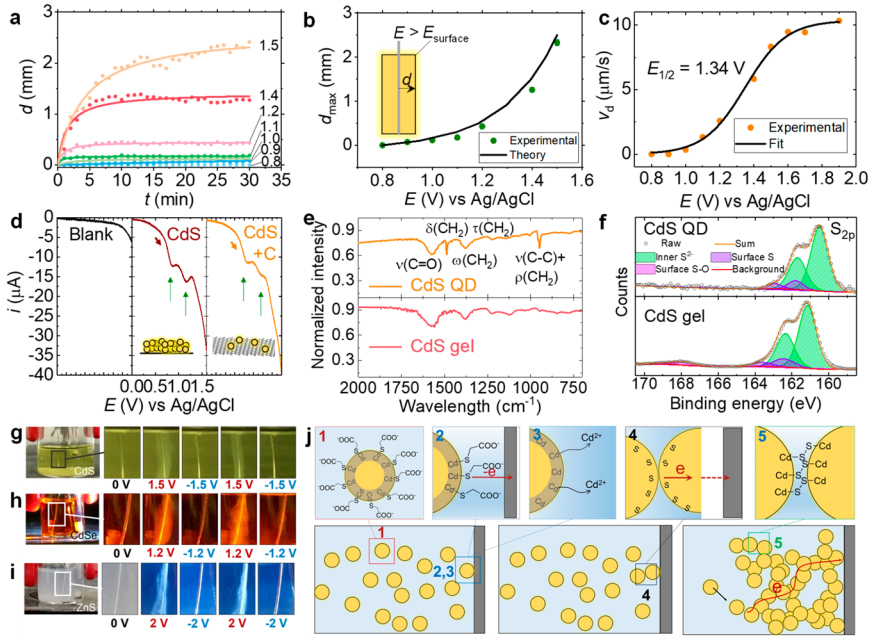

Figure 3. Mechanistic study of electrochemical oxidative gelation. **a**, Gel thickness (d) vs electrogelation time (t) at different electrode potentials (E) vs Ag/AgCl/sat. KCl electrode. **b**, Maximum gel thickness (d_{max}) vs electrode potential (E). **c**, Initial growth rate (v_d) as a function of E. **d**, Linear sweep voltammograms of CdS QDs and CdS QDs supported on carbon (CdS+C). **e**, Fourier transform infrared spectra of CdS QDs and gel. **f**, X-ray photoelectron spectroscopy showing the S_{2p} region of CdS QDs and gel. **g**–**i**, Reversible electrogelation of CdS, CdSe, and ZnS QDs, respectively. **j**, Schematic illustration of electrogelation of CdS QDs. Reproduced with permission from ref 1. Copyright 2020 American Chemical Society.

(Figure 1c,f) followed by an exchange with short-chain thiolate ligands (thioglycolate, TGA). The thiolate groups serve as oxidatively removable "protecting groups" for the QD. Thiolate-capped CdS QDs were dispersed in methanol and subject to electrolysis (Figure 1b). Upon application of a positive potential on the Pt wire, a pale-yellow translucent wet gel immediately formed around the anode (Figure 1b). The microscopic morphology changed from dispersed QDs (Figure 1c,f) to a 3-D pore–matter nanoarchitecture linked by individual randomly oriented QDs (Figure 1d,g), and the macroscopic appearance transformed from an (apparently) homogeneous solution to a monolithic gel (inset, Figure 1c vs 1d). Upon supercritical CO_2 drying, the solvent inside the wet gel was removed, and a free-standing aerogel monolith with volume (inset, Figure 1e) and microstructure (Figure 1h) comparable to those of the wet gel was produced. The CdS QD aerogel exhibits the emissive characteristics of the component QDs upon excitation with a hand-held ultraviolet lamp (Figure 1e).

The CdS QDs electrogelation process does not appear to impact the native structural properties of the QDs or result in sintering or grain growth; the diffraction pattern (Figure 2a) is unchanged with respect to peak position and breadth, with the latter signifying no change in crystallite size, consistent with the electron microscopy results (Figure 1f–h). However, despite the QDs now being connected into a 3-D network, the optical absorption features of the QDs within the assembly change only modestly, with the electrogels exhibiting a small red shift in the first exciton absorption peak positions (Figure 2b) and optical bandgap values (Figure 2c). Recent many-body perturbation theory calculations suggest the minimal changes in optical properties of QD gels relative to QDs arise from changes in the transport gap (associated with interparticle disulfide bond formation) being offset by changes in the exciton binding energy.[21] This is also reflected in the proportional increase in valence band maximum and conduction band minimum as estimated from the combination of UV–vis absorption spectra and ultraviolet photoelectron spectroscopy measurements (Figure 2d). Similar systematic energy level shifts are observed during ligand exchange of QDs,[22] reflecting the important effect of surface ligands and surface structure on the energy levels of the QD. With respect to photoluminescence, both the gel and QDs are dominated by trap state emission (Figure 2e) attributed to the increased probability of non-radiative recombination due to the presence of substantial surface dangling bonds (traps).[6] Critically, the aerogel produced from the QD electrogel exhibits a large specific surface area (220 m^2/g), which suggests we can access more than 50% of the total surface area of the QD components (based on the theoretical surface area for a ~3 nm spherical CdS QD). This access is achieved through interconnected pores with an average diameter of 20.5 nm and cumulative pore volume of 1.2 cm^3/g (Figure 2f).

MECHANISM OF ELECTROCHEMICAL OXIDATIVE GELATION

To determine the mechanism of electrochemical oxidative gelation, we investigated the kinetics and thermodynamics of CdS electrogelation. The electrogelation process, which is hypothesized to proceed via the transport of charge carriers through the gel network formed between the electrode surface and the growth front (Figure 1a), was found to be self-limiting, consistent with a finite conductivity of the QD gel. Thus, the gel thickness (d) increased with electrogelation time (t) until reaching the plateau value (d_{max}) (Figure 3a). As the gel grew, the iR drop in the gel reduced the potential on the gel surface

https://doi.org/10.1021/acs.accounts.3c00042
Acc. Chem. Res. 2023, 56, 1087–1096

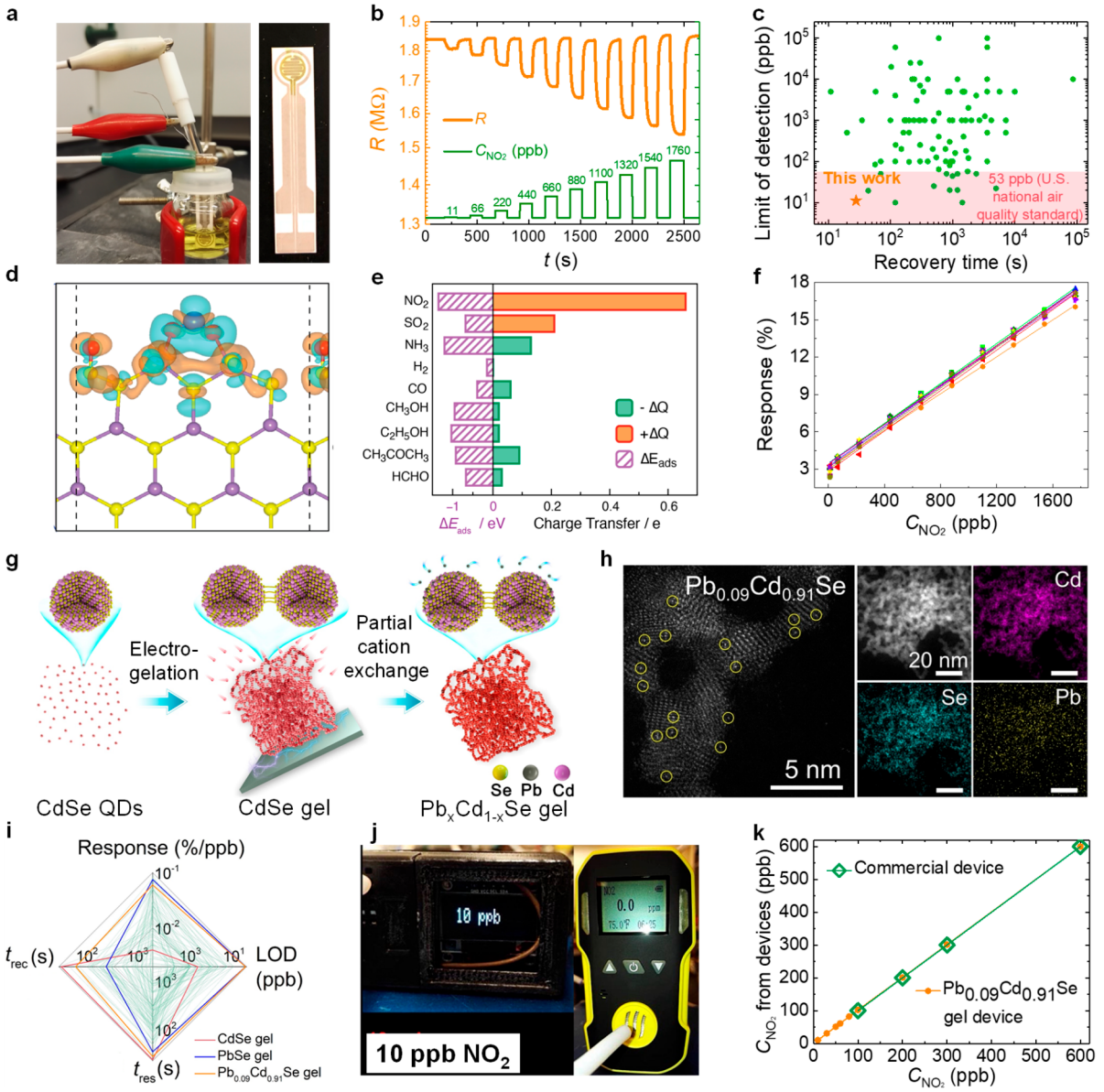

Figure 4. QD gels for gas sensing. **a**, Photograph of the experimental setup for the one-step fabrication of a CdS gel sensor via electrogelation of CdS QDs (left); photographs of a CdS gel sensor (right). **b**, Response−recovery curve of a CdS gel sensor to NO_2 at different concentrations (11−1760 ppb). **c**, Comparison to 100 state-of-the-art room-temperature NO_2 gas sensors in the literature. **d**, Calculated differential valence-electron charge densities of NO_2 adsorption on CdS; charge depletion and accumulation are illustrated by orange and cyan regions, respectively. **e**, Calculated adsorption energies (left) and charge transfer values (right) for different gases on CdS. **f**, Response vs NO_2 concentration plot of 10 independently prepared CdS gel sensors. Reproduced with permission from ref 1. Copyright 2020 American Chemical Society. **g**, Schematic diagram for synthesizing $Pb_xCd_{1-x}Se$ QD gels via cation exchange using different $Pb(NO_3)_2$ concentrations. **h**, HAADF-STEM images and elemental mapping of a $Pb_{0.09}Cd_{0.91}Se$ QD gel. **i**, Comparison between CdSe, PbSe, and $Pb_{0.09}Cd_{0.91}Se$ QD gels and 110 state-of-the-art room-temperature p-type NO_2 gas sensors in the literature. **j**, Photographs of our home-built $Pb_{0.09}Cd_{0.91}Se$ QD gel detector (left) and a commercial NO_2 detector (right) in response to 10 ppb NO_2 at room temperature. **k**, Readouts of the $Pb_{0.09}Cd_{0.91}Se$ QD gel sensor and the commercial NO_2 detector at different NO_2 concentrations. Reproduced from ref 3 under the terms of the CC-BY 4.0 license. Copyright 2021 The Authors, published by Springer Nature.

($E_{surface} < E$), eventually terminating gel growth when the gel became sufficiently thick. The nonlinear relationship between d_{max} and E quantitatively agrees with the theoretical prediction by a simple model considering the iR drop within the gel (Figure 3b). Self-limited gel growth holds great technological promise in film-based applications due to convenient control over film thickness. Furthermore, the initial gel growth rate (v_d) showed a sigmoidal dependence on E (Figure 3c), a characteristic feature for transitioning from a reaction-kinetics-limited process to a diffusion-limited one. This enables us to assign a "standard potential" for CdS QD electrogelation, estimated to be ~1.34 V from the half-wave potential ($E_{1/2}$).

Based on the proposed synthetic pathway for CdS QD electrogelation (Figure 1a), there should be two electro-oxidation steps: (1) oxidative removal of TGA from the QD surface; and (2) disulfide bond formation between QDs.

https://doi.org/10.1021/acs.accounts.3c00042
Acc. Chem. Res. 2023, 56, 1087−1096

Voltammetry experiments (Figure 3d) suggest the corresponding potentials for TGA-capped CdS QDs are 0.8 and 1.2 V, respectively. Consistent with the proposed mechanism, the removal of TGA ligands during electrogelation is confirmed by the weakened bands associated with TGA ligands in the infrared spectrum (Figure 3e). Likewise, the X-ray photoelectron spectroscopy results showed that the gel surface is S-rich whereas the QD surface is Cd-rich, consistent with loss of surface Cd (dissolution) after ligand removal, exposing the sulfide core (Figure 3f). Finally, as the chemical-oxidation-induced process is quasi-reversible, so is electrogelation. Application of a suitable reducing potential led to gel dispersion, consistent with a mechanism of redox-regulated QD assembly and supporting the presence of interparticle disulfide bonds within the gel network (Figures 1a and 3g). Critically, the process can be translated to other metal chalcogenide QDs, as shown by application to CdSe and ZnS QDs in Figure 3h,i. However, the potential required to achieve electrogelation is sensitive to the chemical nature of the metal chalcogenide, with CdSe forming gels at lower potentials and ZnS at higher potentials, relative to CdS. The decreased potential for CdSe is consistent with more facile electrooxidation of selenide relative to sulfide and reflects the thermodynamic redox potentials of the chalcogenide.[23] The requirement of a larger potential for ZnS vs CdS is attributed to differences in the native structure of the two QDs, with ZnS preferentially adopting the cubic zinc blende structure and CdS the hexagonal wurtzite structure.[23]

Taken together, the data are consistent with a three-step electrogelation mechanism, as illustrated in Figure 3j: (1) at an electrode potential >0.8 V, the TGA ligands were oxidatively removed as the QD collides with the anode; (2) after ligand removal, the exposed under-coordinated Cd on the QD surface was solvated and removed, resulting in an S-rich surface; and (3) at an electrode potential above 1.2 V, surface S was further oxidized to form disulfide bonds, crosslinking QDs to yield a gel network. These electrochemical data contribute significantly to our understanding of redox-mediated QD assembly through chemical processes by enabling the redox events to be distinguished and quantified.

ELECTROCHEMICAL GELATION OF QDs MEDIATED BY METAL IONS (NON-COVALENT ASSEMBLY)

QD gels prepared from the electrochemical oxidation of QDs are unstable in reducing environments because the dichalcogenide bonds that link the particles together can be reductively cleaved. Thus, we developed a metal-ion-mediated electrogelation (ME-gelation) approach complementary to the electrooxidative gelation method.[2] Briefly, we applied a positive potential to oxidize a metal electrode (for example, Ni) to release metal ions into the solution containing CdS QDs capped with ligands featuring pendant carboxylate groups, e.g., TGA. The coordination of Ni^{2+} ions by the carboxylate groups triggers the gel growth around the metal electrode. The gap between QD building blocks within the metal-ion-crosslinked QD gel increased when the ligand chain length was increased from C_2 in TGA to C_{11} in mercaptoundecanoic acid (MUA), consistent with linked QDs that are separated by ligand−Ni^{2+}−ligand bonds. The ME-gelation method is compatible with other metals with low oxidation potentials, such as Co, Ag, and Zn, and other QDs of CdSe. In addition, we demonstrated the patterning of QD gels onto printed circuit board chips using ME-gelation, which has potential applications for fabricating QD-based electronic devices such as light-emitting diode displays.

When the applied electrode potential is sufficiently high to drive both oxidative gelation and metal-ion-mediated gelation, we observe interesting electrode-dependent gelation behavior.[20] For Ni electrodes, the gelation is dominated by an oxidative gelation mechanism. We attribute this to the inhibition of metal-mediated electrogelation by disulfide, a byproduct of oxidative electrogelation that binds to the Ni electrode surface and terminates metal ion release. However, for reasons that are not clear to us, disulfide binding to Co, Ag, and Zn does not seem to be a problem, and metal-mediated gelation dominates, regardless of applied potential.

NO_2 GAS SENSING

As alluded to earlier, we are interested in developing metal chalcogenide QD gels prepared by oxidative gelation as high-performance semiconductor gas sensors.[1,3,19] These gels are an ideal platform for gas sensors for the following reasons: (1) the mesoporous architecture of QD gels enables efficient gas exchange throughout the gel network, facilitating interactions between the gas analyte and the QD surfaces and, thus, *rapid response and recovery*;[27] (2) the interconnected structure of the QDs provides facile charge transport for signal transduction; (3) the small crystallite size of QD building blocks within the gel network enables signal transduction because the gas sensitivity increases steeply as the crystallite size decreases to $\leq 2L$, where L is the depth of the space-charge layer (e.g., ∼60 nm for CdS); and (4) the structural properties of QD gels can be conveniently tuned by leveraging the existing chemical toolbox for metal chalcogenide nanocrystal syntheses (e.g., cation exchange, anion exchange, and ligand exchange).[28−32] In contrast, gas sensors that directly use colloidal QDs do not show satisfying performance because the surface ligands of the QDs block adsorption sites and inhibit the electron transport between QDs.

We fabricated CdS gel sensors by one-step electrogelation of CdS QDs on a sensor substrate patterned with interdigitated electrodes (Figure 4a).[1] The CdS gel exhibits exceptional response toward NO_2 with a limit of detection of 11 ppb (Figure 4b), a short response/recovery time (t_{res}/t_{rec}) of <30 s (Figure 4c), a small variation in response of ∼7% during 400 NO_2 exposure/removal cycles, and a superior selectivity toward NO_2. The theoretical calculation shows that NO_2 binds to the Cd sites, causing a significant charge transfer from CdS to NO_2 compared with other gases (Figure 4d,e). Our one-step electrogelation approach not only simplifies the sensor production procedure but also significantly enhances the reproducibility among devices so that 10 independently fabricated gel sensors exhibited a notably low device-to-device variation of <5% (Figure 4f).

However, one limitation of the CdS QD gel sensor is its relatively low response (∼0.01% per ppb NO_2 in Figure 4c). Analysis of NO_2 gas sensors in the literature revealed a trade-off between sensor response and recovery time because a low sensor response is often correlated with weak adsorption of gas analytes on the sensor surface, facilitating desorption and sensor recovery.[3] To overcome this limitation, the positive correlation between charge transfer and adsorption energy must be broken.

We found that Cd ions in CdSe QD gels prepared by oxidative gelation could be partially or fully exchanged by Pb^{2+}

https://doi.org/10.1021/acs.accounts.3c00042
Acc. Chem. Res. 2023, 56, 1087−1096

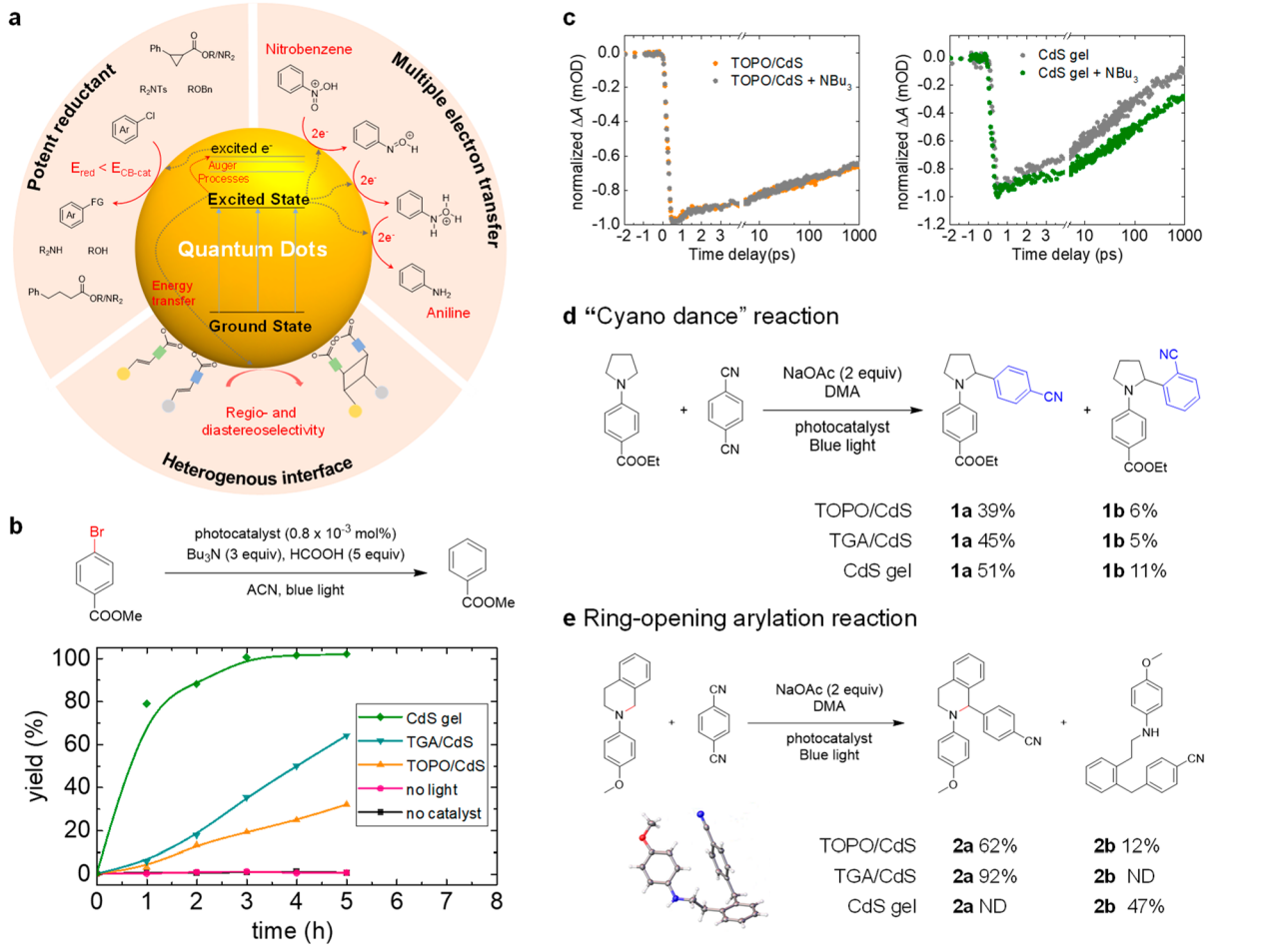

Figure 5. QD gels for photocatalytic organic synthesis. **a**, Schematic representation of the unique photocatalytic reactivities of colloidal metal chalcogenide QDs reported in the literature. **b**, Debromination reaction conditions and the time-dependent yield during dehalogenation of methyl 4-bromobenzoate under no light with the gel (pink) and under blue light with no catalyst (black), TOPO/CdS and TGA/CdS QDs (orange and cyan), and the QD gel (green). **c**, Normalized transient absorption spectra of the bleach recovery with and without the addition of NBu_3 for CdS gel and TOPO/CdS QDs in acetonitrile after 380 nm excitation. **d**, "Cyano dance" reaction and **e**, reductive ring-opening arylation catalyzed by CdS QD gel. The inset on the lower left of panel e is the crystal structure of **2b**. Reproduced with permission from ref 4. Copyright 2022 Royal Society of Chemistry.

by immersing the gel in a Pb^{2+}-containing water/methanol mixture solution (Figure 4g). The gel color gradually changed from the reddish color of CdSe QDs to the black color of PbSe QDs as the extent of cation exchange increased. The distribution of Pb in the $Pb_xCd_{1-x}Se$ gel (x varies from 0% to 100%) evolved as a function of the Pb^{2+} content in the gel. When x was <17%, Pb was atomically dispersed on the gel surface (Figure 4h).[3] The presence of single-ion Pb^{2+} on the $Pb_xCd_{1-x}Se$ QD gel is unexpected because the cation exchange between wurtzite (hexagonal) CdSe QDs and Pb^{2+} typically leads to phase-segregated Janus particles because the thermodynamically stable structure of PbSe is rock salt (cubic).[24−26] We attribute the formation of single-ion decorated QD gels to the unique structural properties of the CdSe QD gel, and in particular, its Se-rich surface.[1,6] The bimetallic gel preserved the large specific surface area and high porosity of the CdSe gel precursor, suggesting that the cation exchange did not cause significant changes to its mesoporous structure. From the NO_2 gas sensing testing, we found that replacing only 9% Cd in CdSe QD gel with Pb (i.e., the $Pb_{0.09}Cd_{0.91}Se$ QD gel) could achieve this goal, leading to the best overall performance of an ultralow detection limit (3 ppb), high response (0.06%/ppb), and short t_{res} (~28 s) and t_{rec} (~60 s) (Figure 4i). The mechanistic study revealed that the atomically dispersed Pb ionic sites in the $Pb_{0.09}Cd_{0.91}Se$ QD gel were responsible for the observed deviation from the conventional correlation between charge transfer and adsorption energy. The $Pb_{0.09}Cd_{0.91}Se$ gel sensor also exhibited pronounced stability and selectivity, with a variation range of only 10% after the 75 h stability test. A wireless portable NO_2 sensor was fabricated using $Pb_{0.09}Cd_{0.91}Se$ gel, and the signals were in line with commercially available NO_2 devices in real-time (Figure 4j,k) but extended to lower detection levels (below the 53 ppb U.S. air quality standard), showing great commercial potential.

PHOTOCATALYTIC ORGANIC SYNTHESIS

Our investigation of QD gels for photocatalytic organic synthesis was motivated by recent studies that demonstrated unusual photocatalytic reactivities of metal chalcogenide QDs, including potent reducing power, the ability to perform multiple electron reductions, and unique regioselectivity and diastereoselectivity (Figure 5a).[33−36] As previously discussed, QD gels retain the confinement characteristics of the QDs but

https://doi.org/10.1021/acs.accounts.3c00042
Acc. Chem. Res. 2023, 56, 1087−1096

lose most of the surface ligands during oxidative electrogelation, which should further improve catalytic performance. We tested this hypothesis using dehalogenation and α-amine arylation reactions as model reactions.[4] The results show that the CdS QD gel exhibited superior photocatalytic activity relative to colloidal QDs (Figure 5b). The initial rate of debromination by a CdS QD gel is 15 times faster than by trioctylphosphine oxide-capped CdS QDs. Spectroscopic results confirm that the high accessibility of surface sites to substrates is responsible for the improved photocatalytic performance of QD gels. Figure 5c shows that after adding the co-reactant Bu_3N, the transient absorption spectra for the QD samples were essentially unchanged. However, the bleach recovery for the CdS gel became slower, indicating that Bu_3N can bind to and thereby passivate surface trap sites on the gel but not on QDs. The gel catalyst is relatively stable and easily recyclable by centrifuging the reaction mixture. The recycled catalyst exhibited similar activity as the fresh catalyst, giving a yield of 70% for α-amino arylation reaction, comparable with the yield of 82% using the fresh catalyst. More excitingly, we discovered two unusual reactivities when developing the substrate scope for the arylation reaction: the "cyano dance" isomerization (Figure 5d) and the reductive ring-opening arylation (Figure 5e). We suspect the "cyano dance" isomerization is caused by the formation of aryl anions during the electron transfer between the ester-bearing substrate and the QDs or QD gel.[37] We think the reductive ring-opening arylation of tetrahydroisoquinolines (THIQ) may be due to strong surface interactions between the QD gel and quaternary ammonium intermediates. However, the detailed mechanisms for the ester-group-enabled "cyano dance" and reductive ring-opening arylation of THIQ are still under investigation.[38−41]

FUTURE DIRECTIONS

We see many exciting future directions for electrochemically driven QD assembly in terms of materials design and applications in sensing and photocatalysis. With respect to the design of new metal chalcogenide gel frameworks, one intriguing possibility is the formation of multicomponent QD gels via potential-controlled electrochemical assembly. For example, the gelation of CdSe QDs proceeds at 1.2 V vs Ag/AgCl/sat. KCl reference electrode, but CdS gelation requires 1.5 V (Figure 3g,h). Intuitively, one might expect that a mixture of CdS and CdSe QDs treated at a potential of 1.2 V would produce gels with only CdSe, and for potentials of 1.5 V and beyond, both CdS and CdSe would be incorporated, with the extent of incorporation depending on the driving potential and the relative concentration of the two components. However, the process appears to be more complex. While we can produce co-gels from mixtures of TGA-capped CdS and CdSe QDs (see preliminary data in Figure 6), we are not yet able to rationally modulate the compositional tuning. Accordingly, one key question we seek to address within the next few years is how to achieve kinetically controlled mixing in multicomponent electrogels? We are also intrigued by the role of the chalcogenide-rich surfaces of the QD gels in mediating cation sorption and exchange pathways, as exemplified by the discovery of Pb^{2+} single-ion sites on CdSe gels partially exchanged with Pb cations, and will probe the extent to which this is universal for other QD gel−cation combinations.

With respect to applications, our results show that QD gels are an efficient transducing platform for converting gas analyte binding to an electrical sensing signal. However, our gas analyte is currently limited to NO_2. How can we modify the QD gels to achieve targeted selectivity toward other gas analytes? Likewise, photocatalytic reactions using QD gels have so far generated many unusual and puzzling results because of our limited understanding of the photodynamics of QD gels and the complexity of the gel catalysts. Accordingly, we will focus on probing the photochemistry of the QD gels, establishing the "right" model reactions, and designing proper control experiments to delineate the unique reactivities of QD gels.

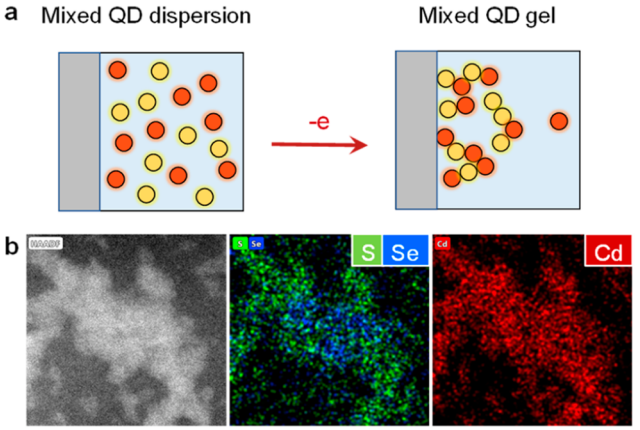

Figure 6. a, Schematic diagram for synthesizing two-component metal chalcogenide QD gels via co-gelation using a mixed QD solution. **b**, HAADF-STEM image and elemental mapping of CdS/CdSe QD gels synthesized by co-gelation approach.

AUTHOR INFORMATION

Corresponding Authors

Stephanie L. Brock − *Department of Chemistry, Wayne State University, Detroit, Michigan 48202, United States;* orcid.org/0000-0002-0439-302X; Email: sbrock@chem.wayne.edu

Long Luo − *Department of Chemistry, Wayne State University, Detroit, Michigan 48202, United States;* orcid.org/0000-0001-5771-6892; Email: long.luo@wayne.edu

Authors

Xin Geng − *Department of Chemistry, Wayne State University, Detroit, Michigan 48202, United States*

Daohua Liu − *Department of Chemistry, Wayne State University, Detroit, Michigan 48202, United States*

Chathuranga C. Hewa-Rahinduwage − *Department of Chemistry, Wayne State University, Detroit, Michigan 48202, United States*

Complete contact information is available at: https://pubs.acs.org/10.1021/acs.accounts.3c00042

Author Contributions

‡X.G. and D.L. contributed equally.

Notes

The authors declare no competing financial interest.

https://doi.org/10.1021/acs.accounts.3c00042
Acc. Chem. Res. 2023, 56, 1087−1096

Biographies

Xin Geng received a B.E. in Material Processing and Control Engineering from Yangzhou University (2013) and a Ph.D. in Engineering Sciences from the University of Mons (2019). He is currently a postdoctoral fellow at Wayne State University in the lab of Long Luo. His current research focuses on the assembly of nanocrystals to design functional materials.

Daohua Liu received a B.E. and M.E. in Environmental Engineering from Changchun University of Technology (2016) and Guangdong University of Technology (2019), respectively. She is a Ph.D. candidate in the Department of Chemistry at Wayne State University in the lab of Long Luo. Her current research studies quantum dot gels as photocatalysts for organic synthesis.

Chathuranga C. Hewa-Rahinduwage completed graduateship examinations in Chemistry from the Institute of Chemistry Ceylon (2012) and received an M.S. in Chemistry from Sam Houston State University (2017) and a Ph.D. in Analytical Chemistry from Wayne State University (2021) under the direction of Long Luo. He is now a senior scientist at TCG GreenChem, Inc.

Stephanie L. Brock is a Professor of Chemistry at Wayne State University. She received her B.S. degree in Chemistry from the University of Washington (1990), where she performed research in the lab of James M. Mayer, and her Ph.D. in Chemistry from the University of California Davis (1995) under the direction of Susan M. Kauzlarich. She worked as a postdoctoral fellow with Steven L. Suib at the University of Connecticut before joining Wayne State University as an Assistant Professor in 1999. She is a Fellow of the AAAS and the ACS, and a member of the Wayne State University Academy of Scholars. She is also an Associate Editor for *Chemistry of Materials* and the Inaugural Deputy Editor for *ACS Materials Au*. Her research efforts are focused on the design of nanomaterials and nanoparticle assemblies for renewable energy, environmental remediation, and sensing.

Long Luo is the Carl R. Johnson Assistant Professor of Chemistry at Wayne State University. He received his B.S. (2009) in Applied Chemistry from Beijing University of Aeronautics and Astronautics and his Ph.D. (2014) in Chemistry from the University of Utah under the guidance of Prof. Henry S. White. Before joining Wayne State University in 2017, he worked as a postdoctoral fellow in the laboratory of Prof. Richard M. Crooks at the University of Texas at Austin. The research goal of his laboratory is to address the grand challenges of our time in the environment, energy, and health by designing, discovering, synthesizing, and utilizing new functional materials and molecules, and by developing novel analytical methods, tools, and devices.

■ ACKNOWLEDGMENTS

L.L., X.G., D.L., and C.C.H.-R. gratefully acknowledge support from NIH (1R35 GM142590-01), DOE (78705), and the start-up funds from Wayne State University. S.L.B. is supported by NSF (DMR-1904775) and DOE (DE-SC0023324)

■ REFERENCES

(1) Hewa-Rahinduwage, C. C.; Geng, X.; Silva, K. L.; Niu, X.; Zhang, L.; Brock, S. L.; Luo, L. Reversible Electrochemical Gelation of Metal Chalcogenide Quantum Dots. *J. Am. Chem. Soc.* **2020**, *142* (28), 12207−12215.

(2) Hewa-Rahinduwage, C. C.; Silva, K. L.; Brock, S. L.; Luo, L. Quantum Dot Assembly Driven by Electrochemically Generated Metal-Ion Crosslinkers. *Chem. Mater.* **2021**, *33* (12), 4522−4528.

(3) Geng, X.; Li, S.; Mawella-Vithanage, L.; Ma, T.; Kilani, M.; Wang, B.; Ma, L.; Hewa-Rahinduwage, C. C.; Shafikova, A.; Nikolla, E.; et al. Atomically dispersed Pb ionic sites in PbCdSe quantum dot gels enhance room-temperature NO_2 sensing. *Nat. Commun.* **2021**, *12* (1), 4895.

(4) Liu, D.; Nyakuchena, J.; Maity, R.; Geng, X.; Mahajan, J. P.; Hewa-Rahinduwage, C. C.; Peng, Y.; Huang, J.; Luo, L. Quantum dot gels as efficient and unique photocatalysts for organic synthesis. *Chem. Commun.* **2022**, *58* (80), 11260−11263.

(5) Rusch, P.; Zámbó, D.; Bigall, N. C. Control over Structure and Properties in Nanocrystal Aerogels at the Nano-, Micro-, and Macroscale. *Acc. Chem. Res.* **2020**, *53* (10), 2414−2424.

(6) Mohanan, J. L.; Arachchige, I. U.; Brock, S. L. Porous semiconductor chalcogenide aerogels. *Science* **2005**, *307* (5708), 397−400.

(7) Arachchige, I. U.; Brock, S. L. Sol−Gel Methods for the Assembly of Metal Chalcogenide Quantum Dots. *Acc. Chem. Res.* **2007**, *40* (9), 801−809.

(8) Saez Cabezas, C. A.; Sherman, Z. M.; Howard, M. P.; Dominguez, M. N.; Cho, S. H.; Ong, G. K.; Green, A. M.; Truskett, T. M.; Milliron, D. J. Universal Gelation of Metal Oxide Nanocrystals via Depletion Attractions. *Nano Lett.* **2020**, *20* (5), 4007−4013.

(9) Sherman, Z. M.; Green, A. M.; Howard, M. P.; Anslyn, E. V.; Truskett, T. M.; Milliron, D. J. Colloidal Nanocrystal Gels from Thermodynamic Principles. *Acc. Chem. Res.* **2021**, *54* (4), 798−807.

(10) Pala, I. R.; Arachchige, I. U.; Georgiev, D. G.; Brock, S. L. Reversible Gelation of II-VI Nanocrystals: The Nature of Interparticle Bonding and the Origin of Nanocrystal Photochemical Instability. *Angew. Chem., Int. Ed.* **2010**, *49* (21), 3661−3665.

(11) Gacoin, T.; Malier, L.; Boilot, J.-P. New transparent chalcogenide materials using a sol− gel process. *Chem. Mater.* **1997**, *9* (7), 1502−1504.

(12) Gacoin, T.; Malier, L.; Boilot, J.-P. Sol−gel transition in CdS colloids. *J. Mater. Chem.* **1997**, *7* (6), 859−860.

(13) Korala, L.; Li, L.; Brock, S. L. Transparent conducting films of CdSe (ZnS) core (shell) quantum dot xerogels. *Chem. Commun.* **2012**, *48* (68), 8523−8525.

(14) Korala, L.; Wang, Z.; Liu, Y.; Maldonado, S.; Brock, S. L. Uniform Thin Films of CdSe and CdSe(ZnS) Core(Shell) Quantum Dots by Sol−Gel Assembly: Enabling Photoelectrochemical Characterization and Electronic Applications. *ACS Nano* **2013**, *7* (2), 1215−1223.

(15) Zambo, D.; Schlosser, A.; Rusch, P.; Lubkemann, F.; Koch, J.; Pfnur, H.; Bigall, N. C. A Versatile Route to Assemble Semiconductor Nanoparticles into Functional Aerogels by Means of Trivalent Cations. *Small* **2020**, *16* (16), e1906934.

(16) Saez Cabezas, C. A.; Ong, G. K.; Jadrich, R. B.; Lindquist, B. A.; Agrawal, A.; Truskett, T. M.; Milliron, D. J. Gelation of plasmonic metal oxide nanocrystals by polymer-induced depletion attractions. *Proc. Natl. Acad. Sci. U. S. A.* **2018**, *115* (36), 8925.

(17) Du, R.; Joswig, J. O.; Hübner, R.; Zhou, L.; Wei, W.; Hu, Y.; Eychmüller, A. Freeze−Thaw-Promoted Fabrication of Clean and Hierarchically Structured Noble-Metal Aerogels for Electrocatalysis and Photoelectrocatalysis. *Angew. Chem., Int. Ed.* **2020**, *132* (21), 8370−8377.

(18) Freytag, A.; Sánchez-Paradinas, S.; Naskar, S.; Wendt, N.; Colombo, M.; Pugliese, G.; Poppe, J.; Demirci, C.; Kretschmer, I.; Bahnemann, D. W.; Behrens, P.; Bigall, N. C. Versatile Aerogel Fabrication by Freezing and Subsequent Freeze-Drying of Colloidal Nanoparticle Solutions. *Angew. Chem., Int. Ed.* **2016**, *55* (3), 1200−1203.

(19) Geng, X.; Liu, X.; Mawella-Vithanage, L.; Hewa-Rahinduwage, C. C.; Zhang, L.; Brock, S. L.; Tan, T.; Luo, L. Photoexcited NO_2 Enables Accelerated Response and Recovery Kinetics in Light-Activated NO2 Gas Sensing. *ACS Sensors* **2021**, *6* (12), 4389−4397.

(20) Hewa-Rahinduwage, C. C.; Silva, K. L.; Geng, X.; Brock, S. L.; Luo, L. Electrochemical gelation of quantum dots using non-noble

https://doi.org/10.1021/acs.accounts.3c00042
Acc. Chem. Res. 2023, 56, 1087−1096

metal electrodes at high oxidation potentials. *Nanoscale* **2021**, *13* (48), 20625−20636.
(21) Aryal, S.; Frimpong, J.; Liu, Z.-F. Comparative Study of Covalent and van der Waals CdS Quantum Dot Assemblies from Many-Body Perturbation Theory. *J. Phys. Chem. Lett.* **2022**, *13* (43), 10153−10161.
(22) Brown, P. R.; Kim, D.; Lunt, R. R.; Zhao, N.; Bawendi, M. G.; Grossman, J. C.; Bulović, V. Energy Level Modification in Lead Sulfide Quantum Dot Thin Films through Ligand Exchange. *ACS Nano* **2014**, *8* (6), 5863−5872.
(23) Davis, J. L.; Chalifoux, A. M.; Brock, S. L. Role of Crystal Structure and Chalcogenide Redox Properties on the Oxidative Assembly of Cadmium Chalcogenide Nanocrystals. *Langmuir* **2017**, *33* (37), 9434−9443.
(24) Lee, D.; Kim, W. D.; Lee, S.; Bae, W. K.; Lee, S.; Lee, D. C. Direct Cd-to-Pb Exchange of CdSe Nanorods into PbSe/CdSe Axial Heterojunction Nanorods. *Chem. Mater.* **2015**, *27* (15), 5295−5304.
(25) Petralanda, U.; De Trizio, L.; Gariano, G.; Cingolani, R.; Manna, L.; Artyukhin, S. Triggering Cation Exchange Reactions by Doping. *J. Phys. Chem. Lett.* **2018**, *9* (17), 4895−4900.
(26) Zhang, J.; Chernomordik, B. D.; Crisp, R. W.; Kroupa, D. M.; Luther, J. M.; Miller, E. M.; Gao, J.; Beard, M. C. Preparation of Cd/Pb Chalcogenide Heterostructured Janus Particles via Controllable Cation Exchange. *ACS Nano* **2015**, *9* (7), 7151−63.
(27) Leventis, N.; Elder, I. A.; Rolison, D. R.; Anderson, M. L.; Merzbacher, C. I. Durable modification of silica aerogel monoliths with fluorescent 2,7-diazapyrenium moieties. Sensing oxygen near the speed of open-air diffusion. *Chem. Mater.* **1999**, *11* (10), 2837−2845.
(28) Gupta, S.; Kershaw, S. V.; Rogach, A. L. 25th Anniversary Article: Ion Exchange in Colloidal Nanocrystals. *Adv. Mater. (Weinheim, Ger.)* **2013**, *25* (48), 6923−6944.
(29) Kovalenko, M. V.; Scheele, M.; Talapin, D. V. Colloidal Nanocrystals with Molecular Metal Chalcogenide Surface Ligands. *Science* **2009**, *324* (5933), 1417.
(30) Kovalenko, M. V.; Bodnarchuk, M. I.; Zaumseil, J.; Lee, J.-S.; Talapin, D. V. Expanding the Chemical Versatility of Colloidal Nanocrystals Capped with Molecular Metal Chalcogenide Ligands. *J. Am. Chem. Soc.* **2010**, *132* (29), 10085−10092.
(31) Anderson, N. C.; Hendricks, M. P.; Choi, J. J.; Owen, J. S. Ligand Exchange and the Stoichiometry of Metal Chalcogenide Nanocrystals: Spectroscopic Observation of Facile Metal-Carboxylate Displacement and Binding. *J. Am. Chem. Soc.* **2013**, *135* (49), 18536−18548.
(32) Lin, Q.; Yun, H. J.; Liu, W.; Song, H.-J.; Makarov, N. S.; Isaienko, O.; Nakotte, T.; Chen, G.; Luo, H.; Klimov, V. I.; Pietryga, J. M. Phase-Transfer Ligand Exchange of Lead Chalcogenide Quantum Dots for Direct Deposition of Thick, Highly Conductive Films. *J. Am. Chem. Soc.* **2017**, *139* (19), 6644−6653.
(33) Jiang, Y.; Wang, C.; Rogers, C. R.; Kodaimati, M. S.; Weiss, E. A. Regio-and diastereoselective intermolecular [2+ 2] cycloadditions photocatalysed by quantum dots. *Nat. Chem.* **2019**, *11* (11), 1034−1040.
(34) Jensen, S. C.; Bettis Homan, S.; Weiss, E. A. Photocatalytic conversion of nitrobenzene to aniline through sequential proton-coupled one-electron transfers from a cadmium sulfide quantum dot. *J. Am. Chem. Soc.* **2016**, *138* (5), 1591−1600.
(35) Huang, C.; Ci, R. N.; Qiao, J.; Wang, X. Z.; Feng, K.; Chen, B.; Tung, C. H.; Wu, L. Z. Direct Allylic C(sp^3)−H and Vinylic C(sp^2)−H Thiolation with Hydrogen Evolution by Quantum Dots and Visible Light. *Angew. Chem.* **2021**, *133* (21), 11885−11889.
(36) Widness, J. K.; Enny, D. G.; McFarlane-Connelly, K. S.; Miedenbauer, M. T.; Krauss, T. D.; Weix, D. J. CdS Quantum Dots as Potent Photoreductants for Organic Chemistry Enabled by Auger Processes. *J. Am. Chem. Soc.* **2022**, *144*, 12229.
(37) Schnürch, M.; Spina, M.; Khan, A. F.; Mihovilovic, M. D.; Stanetty, P. Halogen dance reactions—A review. *Chem. Soc. Rev.* **2007**, *36* (7), 1046−1057.
(38) Kurouchi, H. Diprotonative stabilization of ring-opened carbocationic intermediates: conversion of tetrahydroisoquinoline to triarylmethanes. *Chem. Commun.* **2020**, *56* (59), 8313−8316.
(39) Gui, Y.; Tian, S.-K. Stereospecific Nucleophilic Substitution of Enantioenriched Tertiary Benzylic Amines via in Situ Activation with Benzyne. *Org. Lett.* **2017**, *19* (7), 1554−1557.
(40) Blasko, G.; Elango, V.; Sener, B.; Freyer, A. J.; Shamma, M. Secophthalideisoquinolines. *J. Org. Chem.* **1982**, *47* (5), 880−885.
(41) Maryanoff, B. E.; Almond, H. R. Stereochemistry and conformation of a nitrogen-containing, medium-sized ring: hexahydro-1-phenyl-3-benzazonine derivatives. High 1,4-diastereoselectivity in hydrogenation of an exocyclic alkene. *J. Org. Chem.* **1986**, *51* (17), 3295−3302.

https://doi.org/10.1021/acs.accounts.3c00042
Acc. Chem. Res. 2023, 56, 1087−1096